UNCLASSIFIED
(Approved for Publication)

CLM - P32

EXPERIMENTAL AND THEORETICAL STUDIES OF INSTABILITIES IN A HIGH ENERGY NEUTRAL INJECTION MIRROR MACHINE

by

L.G. Kuo
E.G. Murphy
M. Petravić
D.R. Sweetman

(Submitted for publication in Physics of Fluids)

U.K.A.E.A. Research Group,
Culham Laboratory,
Nr. Abingdon,
Berks.
November, 1963 (C/18 ED)

ABSTRACT

Recent observations with the Phoenix high energy neutral injection experiment are described. At densities where the electron plasma frequency is greater than the ion cyclotron frequency, strong emission at the ion cyclotron frequency and 1/2 the ion cyclotron frequency is observed. This is interpreted on the basis of the theory of electrostatic instability developed by Harris and others. Experimentally, the instability results in strong scattering of ions out of the transverse direction but so far as can be observed, there is no actual loss of plasma. Above a density of 3×10^8 particles/c.c., accumulation of particles is limited by the development of strong low frequency (~ 100 kc/s) oscillations which appear to be an m = 1 displacement of ions and electrons rotating at some fractions of the ion precession frequency. This mode is approximately independent of density. During periods of strong emission at the ion cyclotron frequency, however, another mode is observed, the frequency of which is approximately proportional to density. These observations suggest an m = 1 oscillation driven by a precessional drift instability. The existing theories concerning this low frequency instability are fully discussed. It is found that the effect of finite Larmor radius in the infinite plane plasma calculation is generally negligible at densities below 10^8 particles/c.c. The stability boundary prediction of this calculation when applied to a plasma of cylindrical shape is too low by two orders of magnitude. We present a new calculation in which the mirror field configuration, the cylindrical plasma shape and the associated boundary conditions are fully taken into account. The predicted stability boundary and frequency variation with density are in reasonable agreement with the experiment. The electric field inside the plasma is found to be non-uniform even for the m = 1 mode, so that finite Larmor radius effects are to be expected for this mode, contrary to common belief. The full equation for the electric potential valid for all densities and including the first order finite Larmor radius effect is presented. However, the finite Larmor radius effect is found to be small at densities around 10^8 particles/c.c., and at magnetic fields above 10 kG.

CONTENTS

I. INTRODUCTION

Over the past few years steady improvements in technology have enabled mirror machines using high energy injection to reach higher densities. In reaching densities of the order of 10^8 particles/c.c., new phenomena, including collective phenomena of the plasma as a whole, have been observed.

As is well known, the mirror configuration is unstable, in the simple hydromagnetic theory, to instabilities of the interchange type where the growth of the so-called 'flutes' can cause a loss of plasma to the walls. It is interesting to note that the classical theory of Rosenbluth and Longmire[1] predicts instability at all densities, the growth rate being proportional to $(n)^{\frac{1}{2}}$ at low densities and equal to $(g\,k)^{\frac{1}{2}}$ at high densities, where n is the plasma density, k the wave number of the perturbation and g the equivalent gravitational acceleration. Physically, however, this kind of gross instability is expected to set in only at a density where the Debye length becomes comparable to the typical plasma dimensions, for then electric fields in the plasma can begin to cause collective movements of the ions and electrons. Rosenbluth, Krall and Rostoker[2] (R.K. and R) first modified the theory of Rosenbluth and Longmire to include the effect of finite Larmor radius of the ions. In this case, because of the difference in $\frac{\vec{E} \times \vec{B}}{B^2}$ drift velocities of ions and electrons in the electric field of the perturbation, a stabilization effect results for perturbations of large wave number k at high densities. Extensions of this calculation have been made by Mikhailovskii[3] and later independently by Post to the case where the assumption $n >> \frac{B^2}{4\pi Mc^2}$ was not made. These calculations are more appropriate for the low density plasmas obtained in most high energy mirror machines. It has been shown by Mikhailovskii that the plasma is stable at high densities to disturbances of large wave number k,

just as R.K. and R. have found, but that a region of instability separates this from another region of stability at very low densities. The upper region of stability is obviously of great interest for the achievement of high density thermonuclear plasmas, although it should be remembered that perturbation of small k are still unstable. It is in the context of a high density stable region that Damm, Foote, Futch and Post[4] have interpreted their observation of apparently stable low frequency oscillations in 'Alice' at Livermore.

More complicated modes have been observed in the 'Ogra' machine by Golovin and co-workers[5], although here they seemed able to suppress the growth by the application of 10 kV positive potential on end electrodes.

In the Table Top experiment, Perkins et al[6] have observed at intermediate densities what appears to be an extreme case of an m = 1 instability where the plasma column drifts to the wall while at the same time precessing around the axis. The observations suggest the existence of upper and lower stable regions of density. Experiments of Ioffé et al[7] showed strong flute-like instability in mirror geometry which effectively limited the lifetime of their plasma to some tens of microseconds.

At densities around 10^7 particles/c.c., the electron plasma frequency becomes greater or equal to the ion cyclotron frequency and under such conditions a longitudinal electrostatic wave involving a coupling of axial electron oscillations to ion gyromotion can produce the so-called Harris instability[8,9]. This is characterized by strong coherent emission at the ion cyclotron or related frequencies. Although such instabilities do not cause any movement of the plasma as a whole, they can produce axial scattering and hence possible particle loss. Since this instability originates from the anisotropy in velocity space of the particle distribution

function, which is inherent to some extent in all magnetically confined plasmas, it may prove much more troublesome to eliminate than hydromagnetic instabilities. Observations of strong ion cyclotron oscillations have been reported by workers from the Alice, Ogra and DCX[10] machines. So far no satisfactory method of eliminating this instability has been found.

In our present experiment, the neutral injection Phoenix machine, we have observed low frequency electrostatic oscillations at the surface of the plasma, the frequencies of which are closely related to the grad B precession frequency of the ions in the mirror field. At the same time, ion cyclotron oscillations at the fundamental and half the fundamental frequency have been observed. These phenomena are certainly related to the instabilities discussed above.

II. EXPERIMENTAL APPARATUS

The basic principles of the experimental set-up have been discussed in a previous paper.[11] In Fig.1 is shown a schematic diagram of the main components of the apparatus. A beam of neutral hydrogen atoms obtained by dissociation of 60 keV H_3^+ or H_2^+ ions is injected into a mirror magnetic field perpendicular to the field lines in the median plane. The base pressure in the central chamber is maintained at 10^{-9} Torr by the use of titanium gettering on surfaces cooled to liquid nitrogen temperature. A recent addition to the injector line has been the magnetically driven paddle wheel rotating at 6000 r.p.m. This paddle wheel serves to prevent water molecules from the dissociation chamber from entering the central chamber while leaving the fast neutral atoms relatively unaffected. The pressure in the central chamber is limited by residual gas pressure alone and is not related to the neutral beam intensity which was usually about 8 mA equivalent. At the base pressure of 10^{-9} Torr, the charge exchange loss, which is the main cause of particle loss in the absence of

of instabilities, results in a plasma decay time of approximately 100 milliseconds.

The particles are trapped in the mirror field mainly by the process of Lorentz $\vec{V} \times \vec{B}$ electric field ionization, which is about 300 times more effective than residual gas trapping at pressures of 10^{-9} Torr. At the peak magnetic field of 40 kG, all excited atoms in states with principal quantum number $n > 10$ are ionized. The particles, once trapped, precess about the axis due to the gradient of the magnetic field and hence an axially symmetric plasma is formed. As the Lorentz trapping mechanism ionizes particles at all radii out to 20 cm, the radial extent of the plasma is limited by a scraper probe placed at 8 cm radius. The axial extent of the plasma is determined by the width and divergence of the neutral beam and by the characteristics of the magnetic field. In the present case with a 5 cm diameter neutral beam, the axial extent of the plasma varies between 5.2 cm in the centre to 7 cm at 8 cm radius.

Fig.2 shows a section through the median plane where most diagnostic tools are situated. One of the most important tools consists of an array of CsI scintillation counters collimated by narrow tubes. These counters were used to measure the emission of fast neutral atoms at 0°, 5° and 12° to the median plane. By comparing currents in these directions with those at low densities it is possible to detect small deviations from the expected axial spread of the plasma. Measurement of fast ion current to the scraper gives the number of ions trapped in an annulus just outside the plasma. This was used to calibrate the neutral emission counters in a low density stable regime. The current from the 0° counter, which is far higher than that at other angles, is then used in conjunction with the decay time of the plasma after beam switch off to give an effective measure of plasma density in all regimes. Uncertainties in the knowledge of the secondary emission properties of the scraper probe

and the axial extent of the plasma provide about a factor of two uncertainty in the absolute determination of the plasma density by this method, though relative densities from pulse to pulse are determined with an accuracy of $\pm$ 10%.

An electrostatic probe, which consists of a plate screened from charged particle bombardment but capacitatively coupled to the plasma, was used to measure the plasma surface potential. This probe was coupled to an amplifier the input of which has an integration time constant of 30 ms. At high frequencies, the voltage which appears at the input of the amplifier is the surface potential of the plasma times the ratio of the probe to plasma capacity to input capacity. The capacity of the probe to plasma has been measured using a separate model so that absolute surface potentials can be measured with about a factor of two uncertainty.

The loop aerials shown in the diagram were used in early experiments to detect emission at the ion cyclotron frequency. For the recent experiments, however, ion cyclotron radiation was picked up electrostatically on 90° segments mounted as part of the end plates inside mirror coils. The rest of the end plates were connected to d-c amplifiers to measure end plate currents.

The magnetic field is obtained by electronic integration of the signal from a pick-up coil located at 16 cm radius and is presented digitally to a relative accuracy of 1 part in 10^3.

The signals from various probes and detectors are displayed on a 24 channel oscilloscope which is photographed with a polaroid camera for immediate appraisal. Detailed data for analysis is photographed on moving film using oscilloscopes coupled in parallel with the main display unit.

III. EXPERIMENTAL OBSERVATIONS

The magnetic field pulse used in these experiments rises in

about 1.2 sec. and falls with a similar time constant. The beam was switched off for 100 ms at 1 sec. from the beginning of the pulse so that plasma decay times could be measured at constant magnetic field. Most measurements were taken as a function of magnetic field and density, the latter being varied by changing the injection current or the residual gas pressure. Three distinct regimes occur:

(i) Discontinuous oscillation at the ion cyclotron frequency (~ 60 mc/s at 40 kg).

(ii) Continuous oscillation at the ion cyclotron frequency.

(iii) Strong low frequency (~ 100 kc/s) oscillation.

Strong discontinuous oscillations at ion cyclotron frequencies occur in bursts of 0.1 - 1 ms duration. During this time, a sharp drop in the neutral emission at 0° to the median plane is observed while the 5° or 12° emission remains constant or even rises slightly. There is also a negative current to the end plates and a positive rise in surface plasma potential of a few hundred volts which recovers in a time consistent with the time for replacement of electrons in the plasma. After the burst, the 0° neutral emission gradually recovers in a time corresponding to the build up time of the plasma. These observations are consistent with an electrostatic ion cyclotron resonance instability of the kind described by Harris[9]. In some cases, two frequencies differing by up to 20% are observed simultaneously, and since the magnetic field varies to this extent from the centre to 8 cm radius, it is likely that these short bursts of emission correspond to very localized regions of instability in the plasma. The apparent quenching of the instability is possibly associated with the axial scattering of the particles which may change the anisotropy of the ion-velocity distribution enough to quench the instability.

Fig.3 shows a plot of observed frequency against magnetic field obtained by analysis from a single pulse. In this case, the plasma

radius was limited to 5 cm and consequently the field was uniform to 7% and no simultaneous emission at two slightly different frequencies were observed. However, it is interesting to note the presence of emission at half the ion cyclotron frequency. Preliminary measurement of the phase correlation between two opposite end plate sectors indicate that the signals are in phase at the fundamental frequency, and 180° out of phase at the sub-harmonic frequency.

At lower magnetic fields and in general, higher densities, continuous emission at the ion cyclotron frequency is observed. In this case the oscillation can continue for many tens of milliseconds. Continuous axial scattering of ions occurs until a quasi-stable situation is reached. In this case the instability possibly extends over a much larger region of the plasma than is the case for discontinuous emission.

Attempts to increase the plasma density above 3×10^{8} particles/c.c. result in a new and radically different phenomenon. Strong low frequency oscillations appear on the electrostatic probe which correspond to potentials at the surface of the plasma of a kilovolt or more. If the beam is switched off at this stage these persist even when the density has fallen far below the critical value. These oscillations often appear to be triggered by a burst of discontinuous ion cyclotron emission. In cases where it is not triggered, rise times of 5 ms or more have been observed.

The frequency of these oscillations is normally locked to about half the ion precession frequency calculated for the outer radius of the plasma and is independent of density. Occasionally the frequency drops to a lower value. When in this mode of oscillation, the frequency appears to be approximately proportional to density. The transition between the density-independent higher frequency and the density-dependent lower frequency mode is often continuous. And

significantly, the lower frequency mode is always accompanied by intense discontinuous or continuous ion cyclotron frequency oscillations.

Fig.4 shows the frequencies observed for a single pulse plotted as the ratio of observed frequency ω to precession frequency Ω, against 1/B. The two modes and the gradual transition between them are clearly seen. Since the precession frequency is proportional to ion energy, measurements have been made at 30 keV and 20 keV, and Fig.5 shows that the observed frequencies change in the expected way. The branch at low magnetic fields for the 30 keV case shows also a gradual transition to the lower frequency mode.

As the correlation of ion cyclotron emission with the lower frequency oscillations is a rather unusual feature, results from five pulses are collected and shown in Fig.6 where it may be seen that the change in frequency is related to the intensity of ion cyclotron emission.

By correlating signals from two electrostatic probes 135° apart in azimuth, it has been established that both the higher frequency and lower frequency precession modes represent an m = 1 charge distribution rotating in the direction of the ion precessional drift. Observations of the neutral emission at the onset of these oscillations show approximately equal drops at the three angles of 0°, 5° and 12° to the median plane. These facts suggest an eccentric precession of the plasma, as expected from an m = 1 flute instability, which then causes large plasma loss to the scraper probe. The potential appearing on the electrostatic pick-up probe varies approximately sinusoidally with time which suggests that the configuration corresponds to a small displacement of two cylindrical charge distributions.

By superposing results from many pulses, it has been possible to

build up a general picture of regions on the density vs magnetic field plot where certain instabilities occur. Fig.7 shows the path of many pulses where discontinuous and continuous ion cyclotron emission occur. It may be seen that all emission occurs above the line $\omega_p = \omega_c$ where ω_p is the electron plasma frequency and ω_c the ion cyclotron frequency, and that continuous emission tends to occur at lower magnetic fields. Similarly it has been possible to compile the points during the magnetic field pulse at which the flute instability starts. This is shown in Fig.8. It is to be noted that there is a strong dependence on magnetic field and that below about 15 kG the plasma is apparently stable at least up to the density investigated. It should be noted that since the magnetic field is pulsed, the plasma is present for only about 200ms at fields below 18 kG, and for longer times at higher fields. The observed effect may possibly be connected with this varying time, that is to say that the plasma may remain stable for longer periods at lower densities. This point will be settled by further experiments.

Fig.9 is a schematic diagram of the results of Figs. 7 and 8 combined.

It is interesting to ask to what extent the presence of these instabilities limit the densities attainable in the present system. From a series of pulses where the injection current, j, was kept constant while the residual gas pressure was progressively lowered, it has been possible to obtain a plot of density at a fixed magnetic field against plasma decay time constant τ. In the absence of all but the charge exchange loss, the ion density n^+ is given by:-

$$n^+ = \frac{1}{n_o v \sigma} \frac{dn^+}{dt}$$

$$= \tau \frac{dn^+}{dt} \propto \tau j$$

therefore the density should be directly proportional to τ. As may

be seen in Fig.10, at densities below 3×10^8 particles/c.c., this is indeed so; but above this attempts to increase density result in the appearance of "flutes" whose amplitude increases with τ with little change in density. Preliminary results of applying potentials between 1 - 10 kV on the end plates, as in the Ogra experiment, show that indeed higher densities may be obtained with potentials > 3 kV (see Fig.10). However the low frequency oscillations are by no means suppressed and the wave forms become much more complex and irregular. These measurements on the effect of end plate potentials are still at an early stage and will not be discussed further in this paper.

IV. DISCUSSION

A. ELECTROSTATIC INSTABILITY

It has been shown by Harris[9] that longitudinal electrostatic oscillation in a high-temperature low-density plasma may be unstable if the velocity distributions of ions and electrons are sufficiently anisotropic. In the calculation the Vlasov equation together with Maxwell's equations: $\nabla.E = 4\pi e\int f d^3V$ and $\nabla \times E = -\frac{1}{c}\frac{\partial B}{\partial t} = 0$ are used; and by assuming different initial distribution functions, f, different results are obtained. Harris has calculated the case when the ion and electron velocity distributions are of the form $f \propto \delta(V_{\parallel}) \exp -\left(\frac{V_{\perp}^2}{\alpha_{\perp}^2}\right)$, that is there is a spread of velocities in the direction perpendicular to the magnetic field and zero velocity parallel to the magnetic field, and hence the ratio of perpendicular to parallel energy $T_{\perp}/T_{\parallel}$ is effectively infinite. In this case, oscillations are found at frequencies $\omega = \ell\omega_c$ where ℓ is any integer and ω_c the ion cyclotron frequency. These oscillations are unstable if:-

$$\frac{k_{\parallel}^2}{k^2}\frac{\omega_p^2}{\omega_c^2}\left(\exp\left(-\frac{\alpha_{\perp e}^2 k_{\perp}^2}{2\omega_{ce}^2}\right) I_o\left(\frac{\alpha_{\perp e}^2 k_{\perp}^2}{2\omega_{ce}^2}\right)\right) > \ell^2$$

where k is the wave number, $k_{\parallel}$ and $k_{\perp}$ components of k parallel and perpendicular to the magnetic field, and ω_{ce} the electron cyclotron frequency. From this it may be seen that the most unstable wave is where $\ell = 1$ and k_z is close to k. The instability condition then reduces to the familiar form $\omega_p > \omega_c$.

Since the unstable wave is in part propagating parallel to the magnetic field, it may be expected that a spread in velocities in the parallel direction might produce a Landau damping effect and relax the instability condition. Recently Kahn[12] has made calculations on the same lines as Harris but assuming instead that the electrons have zero velocity and that the ion distribution function is of the form:-

$$f_i = \exp \frac{-1}{2\sigma^2} \left(V_{\parallel}^2 + \frac{V_{\perp}^2}{M^2}\right)$$

$$M^2 = \frac{T_{\perp}}{T_{\parallel}} .$$

Interesting results are obtained in that the frequencies of unstable waves are found to be in the region:-

$$(S + \tfrac{1}{2})\ \omega_c < \omega < (S + 1)\ \omega_c$$

where S is an integer $\geqslant 0$. The instability condition is $\omega_p > (S + 1)\ \omega_c$ and instability exists between the Sth and $(S + 1)$th resonance only if $(S + 1) \leqslant \frac{1}{2} \frac{T_{\perp}}{T_{\parallel}}$. Therefore for the most unstable case, $S = 0$, $T_{\perp} = 2T_{\parallel}$. These results do not however imply that there would be an unstable wave at $\omega = \frac{1}{2}\ \omega_c$. A very recent calculation by Dnestrovsky et al[13] assuming Maxwellian distributions for both ions and electrons in transverse and perpendicular directions has given similar results. Giving the electrons some temperature allows stability for higher values of anisotropy, that is $\frac{T_{\perp i}}{T_{\parallel i}} >> 2$. It is interesting to note also that the growth rate for the wave at $\omega = \frac{1}{2}\ \omega_c$ is found to be negligible compared to that at $\omega = \omega_c$. Therefore the reason for our observation of emission at $\omega = \frac{1}{2}\ \omega_c$ has to be sought elsewhere.

B. LOW FREQUENCY DRIFT INSTABILITY

1. Survey

It is well known that magnetohydrodynamics predict interchange instability for plasmas in simple mirror magnetic field configurations with a growth rate of $\omega_H = (g\,k)^{\frac{1}{2}}$, where g is an effective centrifugal acceleration and k is the wave number of the perturbation. The magnetohydrodynamic approximation, however, breaks down for slow growth rates, when $\frac{\omega_H}{\omega_c}$, becomes comparable to $(k\,a)^2$, the square of the product of wave number with ion Larmor radius.

The effects of a finite Larmor radius, which becomes very important when $(k\,a)^2 = \frac{\omega_H}{\omega_c}$, have been studied by many authors. The papers most relevant to our experiment are those of R.K and R, Krall and Rosenbluth[14, 15, 16], and Mikhailovskii[3]. R.K. and R. have treated the case of a low β, infinite, inhomogeneous plasma using the collisionless Boltzmann equation under the condition that plasma density $n >> \frac{B^2}{4\pi Mc^2}$, where B is the magnetic field and M the ion mass. The magnetic field was assumed to be constant apart from the small inhomogeneity caused by currents whose effect was shown to be negligible. It was shown that for large enough wave number such that $(k\,a)^2 > \frac{\omega_H}{\omega_c}$, where ω_H is the hydrodynamic growth rate, stabilization results. In this calculation it was assumed that the electric vector associated with the oscillation was parallel to the direction of propagation of the wave. The authors call this the "longitudinal and electrostatic" approximation. The recent calculation of Krall and Rosenbluth[16] allows for the possibility of the existence of both components of the electric field perpendicular to the direction of propagation. Although the 'longitudinal' mode is still found to be a particular solution of the general problem, there is also a mixed mode and a purely transverse mode. The mixed mode contains the electric field perpendicular to the zero order magnetic field, while the transverse mode contains only the electric field component

parallel to the magnetic field. The mixed mode is found to be oscillatory and stable to the order $(k\,a)^4$, while the transverse mode is found to be unstable at frequencies $\omega = - k v_D$ and $\omega = - k \frac{v_D}{\beta}$ where v_D is the ion drift velocity and β is the usual ratio of plasma pressure to magnetic field pressure. For small values of β, the growth rates for these waves are found to be extremely small.

The earlier paper of R.K.and R. also treats the case of cylindrical geometry and applies the results to mirror machines. The mirror configuration was taken into account by introducing an equivalent gravitational force with the components in Cartesian coordinates $[\frac{mv^2}{R} \frac{x}{r_o}, \frac{mv^2}{R} \frac{y}{r_o}, 0]$. This was taken to represent the effect of the inhomogeneity of the magnetic field, which was otherwise assumed constant. The effect of the finite Larmor radius was again found to be a stabilizing one for all harmonics of the potential $\overline{\Psi} = r^m e^{im\phi}$ except for m = 1. For the latter mode, there is no stabilization whatever. The physical explanation offered was that since the electric field is uniform, the ion and electron drifts caused by the electric field are the same and the size of the Larmor orbit is irrelevant. The growth rate for the m = 1 mode was found to be $(g\,k)^{\frac{1}{2}}$, exactly as in magnetohydrodynamics. However, it is to be noted that the solution $\overline{\Psi} = r^m e^{im\phi}$ was obtained with the assumption that the magnetic field was constant throughout. It has already been pointed out that the calculations of R.K. and R. assumed $n >> \frac{B^2}{4\pi Mc^2}$. As this corresponds to $n >> 5 \times 10^9$ particles/c.c. for B = 10 kG, their theory is not applicable to the conditions in the presentday high energy injection mirror machines.

The problem of a non-uniform infinite plasma in a constant magnetic field has recently been treated by Mikhailovskii, whose calculation is not restricted to any particular density range. Two ion velocity distributions have been considered and the ion cyclotron motion was taken into account. The dispersion relation, for

a Maxwellian velocity distribution, in the high density limit takes the form:-

$$\omega^2 - \tfrac{1}{2}\left(\frac{\kappa k \bar{V}^2}{\omega_c}\right)\omega + g\kappa = 0 \qquad \ldots\ (1)$$

for

$$\frac{k^2\bar{V}^2}{\omega_c^2} << 1$$

where $\kappa = \frac{1}{n}\frac{dn}{dr}$ the relative density gradient, and $\bar{V}^2$ the mean square of the ion thermal velocity. The condition $\frac{k^2\bar{V}^2}{\omega_c^2} << 1$ is satisfied for the longest wavelengths in most experiments. The resulting stability condition is identical with that of R.K. and R. For large enough values of k such that:-

$$\frac{16\omega_c^2}{\kappa k^2(\bar{V}^2)^2}\, g \leqslant 1 \qquad \ldots\ (2)$$

stabilization results. Otherwise, for small k's which do not satisfy this condition, the plasma is unstable with the growth rate $(\kappa g)^{\frac{1}{2}}$. Without the finite Larmor radius term, the plasma would be unstable for all $n >> \frac{B^2}{4\pi Mc^2}$ with growth rate $(g k)^{\frac{1}{2}}$.

For low densities, the dispersion relation takes the form:-

$$\omega^2 + \omega\left[\frac{gk}{\omega_c} - \frac{\kappa k\bar{V}^2}{2\omega_c}\frac{4\pi Mc^2}{B^2}n\right] + g\kappa\frac{4\pi Mc^2}{B^2}n = 0 \qquad \ldots\ (3)$$

This relation, in a slightly different form, has also been obtained by Post[4]. For very low densities the second term in the square bracket is much smaller than the first:-

$$|g| >> \frac{|\kappa|\bar{V}^2}{2}\frac{4\pi Mc^2}{B^2}n$$

This is satisfied for example for densities below 10^8 particles/c.c. if the mean particle energy is about 20 keV, the drift velocity is 10^6 cm/sec and the magnetic field is greater than 10 kG. In this case the finite Larmor radius effect is negligible as it manifests itself only in the term containing $\bar{V}^2$. In fact, it does not become really important until the above inequality is reversed. Under the listed conditions the stability condition becomes:-

$$\frac{16\pi c^2 \kappa}{Mgk^2} n \leq 1 \qquad \ldots\ldots (4)$$

One can now try to apply this plane geometry result to a plasma of cylindrical shape by setting

$$m\frac{gk}{\omega_c} = \Omega = \frac{e}{e} T \frac{1}{B^2}\frac{dB}{dr} \text{ , and } k = \frac{m}{r_o}$$

where T is the thermal ion energy, r_o the plasma radius and m is the mode. From (4), we then obtain:-

$$\frac{16\pi e^2 r_o \kappa n}{m^{\nu} T \frac{1}{B}\frac{dB}{dr}} \leq 1 \qquad \ldots\ldots (5)$$

Once unstable, the growth rate is $(g\kappa \frac{4\pi Mc^2}{B^2} n)^{\frac{1}{2}}$.

It is evident that the procedure by which the above transformation is obtained is highly unsatisfactory. The electric field in the cylindrical geometry becomes purely azimuthal which is certainly not the case. By assuming a large Ω , one implicitly assumes a highly non-uniform magnetic field, while the calculation assumes a constant magnetic field throughout. Nevertheless, the stability condition resulting from the full equation (3), with the appropriate values for the parameters, has been compared with the experimental results on a density vs magnetic field plot as shown in Fig.13. The strong dependence of the theoretical stability boundary on the magnetic field enters indirectly through the density gradient because of the way the plasma edge is defined in Phoenix; as the scraper probe removes particles over one Larmor diameter, the most reasonable assumption is:-

$$\kappa = -\frac{1}{2a}$$

It may be seen that the theoretical stability boundary is lower by two orders of magnitude than the experimentally found boundary. It would appear then that the plane geometry calculation when applied in this way to cylindrical geometry is grossly unsatifactory.

To explore the possibility of the existence of an upper high density stable region for m = 1 in cylindrical geometry, one again performs the same transformation on relation (2) and obtains the result that the plasma will be stable at high densities provided

$$\frac{8r_o^3 \frac{dB}{dr}}{m^2 \kappa a^2 B} \leqslant 1.$$

This relation is extremely difficult to satisfy for most plasmas in mirror geometry and it is certainly not satisfied in Phoenix.

From the foregoing discussion, it may be seen that a theory treating the mirror magnetic field correctly and taking into account the finite size of the plasma at least in the direction perpendicular to the magnetic field would be highly desirable. Such an approach has been made and will be described in the following paragraphs*

2. Calculation for mirror geometry

The Poisson equation in cylindrical co-ordinates (r, ϕ, z) is used:-

$$-\nabla^2 \underline{\Psi} = 4\pi ec\,(n_i' - n_e')$$

where $\underline{\Psi}$ is the electrostatic potential considered to have the form $\underline{\Psi} = \psi(r)\exp(i\omega t + im\phi)$ and n_i' and n_e' are the perturbations in ion and electron densities of the form $n' = n'(r)\exp(i\omega t + im\phi)$ The perturbations n_i' and n_e' are calculated from the linearized continuity equation:-

$$\frac{\partial n'}{\partial t} + \vec{v}_o \cdot \nabla n' + \vec{v} n_o + n_o \,\mathrm{div}\, \vec{v}' = 0$$

where $n_o(r)$ is the unperturbed density distribution. The zero order velocity is taken to be equal to the drift velocity due to the magnetic field gradient:-

---

* This approach was suggested and outlined to us by W.B. Thompson.

$$\vec{v}_o = \vec{v}_D = \vec{\phi}_o \frac{c}{e} \frac{T}{B^2} \frac{dB}{dr} , \quad \nabla \cdot \vec{v}_o = 0$$

The magnetic field is defined to have the form:-

$$\vec{B} = \vec{z}_o B(r) = \vec{z}_o \frac{B_o}{1 + B_1 r^2}$$

This type of magnetic field dependence on r produces very conveniently a precessional drift frequency which is independent of the co-ordinates:-

$$\Omega = \frac{|\vec{v}_D|}{r} = - \frac{c}{e} T \frac{2B_1}{B_o}$$

The perturbed velocity $\vec{v}'$ is determined by the drifts due to the oscillating electric field:-

$$\vec{v}' = \frac{\vec{E} \times \vec{B}}{B^2} + \frac{D}{Dt} \left(\frac{\vec{E}}{B\omega_c}\right)$$

$$= \frac{\vec{E} \times \vec{B}}{B^2} + \frac{(\frac{\partial}{\partial t} + \vec{v}_D \cdot \nabla) \vec{E} \, Mc}{e B^2}$$

where

$$\vec{E} = - \nabla \underline{\Psi}$$

By using $(\vec{v}_D \cdot \nabla)\vec{E}$ where $\vec{v}_D$ is only the guiding centre motion, the finite Larmor radius effect is not taken into account; this effect will be treated separately in section 3.

With the above assumptions, the calculation of n_i' and n_e' is straightforward. Restricting the calculation to the case $\beta << 1$, to low frequencies $\frac{\omega}{\omega_c} \approx \frac{\Omega}{\omega_c} << 1$, and neglecting the electron drift in the magnetic field $\Omega_e << \omega \approx \Omega$, the following equation for the electrostatic potential is obtained:-

$$\frac{d^2\psi}{dr^2} + \left[\frac{1}{r} + \frac{4\pi Mc^2}{B^2} \frac{dn_o}{dr} \frac{(1-2\delta)}{\varepsilon}\right] \frac{d\psi}{dr} + \left[\frac{-4\pi ecm^2\Omega}{\omega(\omega + m\Omega)B} \frac{dn_o}{dr} \frac{(1-2\delta)}{\varepsilon r} - \frac{m^2}{r^2}\right] \psi = 0 \quad \ldots . (6)$$

where

$$\varepsilon = 1 + \frac{4\pi Mc^2}{B^2} n_o, \text{ and } \delta = \frac{\nabla \ln B}{\nabla \ln n_o}$$

Before this equation is simplified to apply to the low density regime, we would like to compare this equation with the result of R. K and R. We therefore set m = 1 and $\psi = r$ (which implies a uniform electric field) in equation (6) and obtain:-

$$\frac{Mc^2}{B} - \frac{ec\Omega}{\omega(\omega + \Omega)} = 0$$

It may be seen immediately that this can be a dispersion relation only if B is constant, contrary of course to the assumption Ω = constant. If, however, one does make this inconsistent assumption, we then get the usual magnetohydrodynamic result that the growth rate

$$\omega_H = (\Omega\ \omega_c)^{\frac{1}{2}} = (g\ k)^{\frac{1}{2}}$$

It may be concluded therefore that if the magnetic field variation in mirror geometry is taken into account properly, then the internal electric field cannot be uniform even for the m = 1 mode. In consequence, the conclusion that the finite Larmor radius effect is non-existent for the m = 1 mode, for all densities, does not appear to be correct.

The differential equation (6) has not yet been solved for all densities. However for densities below 10^9 particles/c.c. and magnetic fields above 10 kG, $\frac{4\pi Mc^2}{B^2} n_o << 1$ and equation (6) can be reduced to a Bessel's equation provided certain reasonable density distributions are chosen.

Equation (6) for low densities takes the form:-

$$\frac{d^2\psi}{dr^2} + \frac{1}{r}\frac{d\psi}{dr} + \left[\frac{-4\pi ecm^2\Omega}{\omega(\omega + m\Omega)B}\frac{dn_o}{dr}\frac{(1 - 2\delta)}{r} - \frac{m^2}{r^2}\right]\psi = 0 \qquad \ldots.(7)$$

This equation with $\delta = 0$ was obtained by Kadomtsev[17] and solved assuming B = constant. We require $\frac{dn_o}{dr}\frac{(1 - 2\delta)}{Br}$ = constant. This may be satisfied by a density distribution of the following form:-

$$n_o(r) = \frac{N_o}{(1 + B_1 r_o^2)^2 - 1}\left[\frac{(1 + B_1 r_o^2)^2}{(1 + B_1 r^2)^2} - 1\right] \qquad \ldots.(8)$$

where r_o is the plasma radius at which the density is zero, and N_o is the plasma density at r = 0. This density distribution is shown in Fig.11 by the curve marked $n_o I$. For this density distribution, the solution for the potential inside the plasma boundary is $A\, J_m(\alpha r) \cos m\phi$ where α is defined by:-

$$\alpha^2 = \frac{-16\pi ecm^2\Omega}{\omega(\omega + m\Omega)} \quad \frac{B_1 N_o}{B_o[1 - (1 + B_1 r_o^2)^2]} \qquad \ldots\ (9)$$

The dispersion relation is obtained by requiring that the radial and azimuthal electric fields be continuous across the boundary at $r = r_o$. The electric fields for $r > r_o$ are given by:-

$$E_r = C \frac{\cos m\phi}{r^2} \ , \ E_\phi = C \frac{m \sin m\phi}{r^2}.$$

The boundary condition then requires:-

$$(m - 1)\ J_m(\alpha r_o) = \alpha r_o\ J_{m-1}(\alpha r_o) \qquad \ldots\ (10)$$

Equation (10) gives the following dispersion relation:-

$$\frac{\omega}{\Omega} = \frac{-m}{2}\left\{1 \pm \left[1 - \frac{32\pi e^2 r_o^2}{Z_m T[(1 + B_1 r_o^2) - 1]} N_o\right]^{\frac{1}{2}}\right\} \qquad \ldots\ (11)$$

where

$$Z_m = 5.76 \text{ for } m = 1$$
$$= 12.68 \text{ for } m = 2 \text{ etc.}$$

The frequency $\frac{\omega}{\Omega}$ has a parabolic dependence upon density N_o and this is shown in Fig.12. It is interesting to note that the frequencies at which the unstable oscillations may be observed are $\frac{\omega}{\Omega} = \frac{-m}{2}$ The minus sign means that the wave is travelling in the same direction as the ion. Also shown is the prediction from the theory of Mikhailovskii as given by equation (3) used with the appropriate cylindrical geometry parameters. It has the same functional dependence as the other calculation because at these low densities finite Larmor radius effect is negligible. The stability condition given by equation (11) is the following:-

$$N_o \leq 6{,}85 \times 10^7 \text{ particles/c.c.}$$

for the following characteristic Phoenix parameters:-

$$B_1 = .004$$

$$\varepsilon = 20 \text{ keV}$$

$$r_o = 8 \text{ cm}$$

It would now be interesting to see how much this stability condition is dependent on the radial density distribution. The density gradient assumed in this calculation is smaller than any encountered in the experiment for fields greater than 5 kG. As has already been mentioned, the density profile in Phoenix can be better approximated by a curve similar to n_oII in Fig.11. The value $(r_2 - r_1)$ is given by one Larmor diameter and hence is inversely proportional to magnetic field. The equation for the electric potential can now be written from equation (7) for the three distinct regions:-

$r < r_1$ $\qquad \dfrac{dn_o}{dr} = 0 \qquad \dfrac{d^2\psi}{dr^2} + \dfrac{1}{r}\dfrac{d\psi}{dr} + (\gamma^2 - \dfrac{m^2}{r^2})\,\psi = 0$

$$\gamma^2 = \frac{4\pi ecm^2\Omega}{\omega(\omega + m\Omega)} \frac{dB}{dr} \frac{2N_o}{B^2 r} = \text{constant} \qquad \ldots\ (12a)$$

$$\psi = A\, J_m(\gamma r)$$

$r_1 < r < r_2$ $\qquad \dfrac{d^2\psi}{dr^2} + \dfrac{1}{r}\dfrac{d\psi}{dr} + (\alpha^2 - \dfrac{m^2}{r^2})\,\psi = 0$

$$\alpha^2 = \frac{-4\pi ecm^2\Omega}{\omega(\omega + m\Omega)B} \frac{dn_o}{dr} \frac{(1 - 2\delta)}{r} = \text{constant} \qquad \ldots\ (12b)$$

$$\psi = D_1 J_m(\alpha r) + D_2 N_m(\alpha r)$$

$r > r_2$ $\qquad \dfrac{d^2\psi}{dr^2} + \dfrac{1}{r}\dfrac{d\psi}{dr} - \dfrac{m^2}{r^2}\,\psi = 0 \qquad \ldots\ (12c)$

$$\psi = \frac{C}{r}$$

where A, D_1, D_2, and C are constant co-efficients, and J_m and $\underline{N}_m$ are Bessel and Neumann functions of order m respectively. The boundary problem can again be solved by matching the radial and tangential electric fields at $r = r_1$, and $r = r_2$. This gives the following relation for m = 1.

$$-\frac{\alpha}{\gamma} J_1(\gamma r_1) \left[J_o(\alpha r_2) \underline{N}_o(\alpha r_1) - J_o(\alpha r_1) \underline{N}_o(\alpha r_2) \right]$$

$$= J_o(\gamma r_1) \left[J_1(\alpha r_1) \underline{N}_o(\alpha r_2) - J_o(\alpha r_2) \underline{N}_1(\alpha r_1) \right] \quad .... (13)$$

This was solved numerically[18] for αr_1, and the dispersion relation obtained. The results are plotted in Fig.13 where a stability boundary for various magnetic fields is shown. As the density gradients taken are all steeper than in the case of profile n_o I, the stability boundary lies just below the value $N_o = 6.85 \times 10^7$ particles/c.c. This confirms the expectation that the plasma is more stable for smaller density gradients.

Since experimentally the plasma is observed to be unstable above about 2×10^8 particles/c.c., the predictions of this calculation are only about a factor of four down and this may be considered quite satisfactory. It should be pointed out that we have assumed the precession frequency Ω to be constant throughout the calculation, while in Phoenix the precession frequency rises with radius and at 8 cm is about 1.5 times the value used in this calculation. This is because while the magnitude of B is quite well represented by the simple analytical form $B = \frac{B_o}{1 + B_1 r^2}$, $B_1 = .004$, the gradients of B at large values of r are not.[1] The exact effect of the variation of precession frequency on the stability boundary is unknown, but if one assumes that the value of the precession frequency at the plasma boundary is the most important one, then the present calculated stability boundary may be raised by 50%. The effect of considering a plasma cylinder of finite lengths with the

appropriate boundary conditions rather than an infinite one may also change somewhat the stability boundary*.

It is interesting to interpret the experimental observations in terms of the dispersion relation given in equation (11) and expressed graphically in Fig.12. This dispersion relation predicts stable oscillations for low densities below some critical value. For higher densities an unstable rotation occurs at a frequency equal to half the ion precession frequency. This is consistent with the experimental observations although it is important to note that the value of Ω used to normalize the experimental results is that calculated for the edge of the plasma; the central value being some 50% lower. In practice, the presence of the scraper probe limits the maximum radial extent of the plasma and attempts to increase the density result in increased separation of the ions and electrons which results in increased electric fields but little increase in density. The separation of the ion and electron clouds necessary to explain the experimental result is of the order of 1 cm to be compared with a plasma radius of 8 cm. This is consistent with the near sinusoidal azimuthal variation of potential of 1 kV observed experimentally.

Switching the beam off results in an exponential decay of plasma density and amplitude of the sinusoidal electrostatic probe signal. The frequency of the signal remains either nearly constant to $\pm$ 20% or decreases approximately linearly with density over at least an order of magnitude. This is to be compared with the prediction of equation (11) which suggests the possibility of two modes, the upper increasing towards the ion precession frequency and the lower decreasing towards zero frequency, as the density is reduced.

It is difficult to make detailed predictions of the exact motion

* A treatment of this effect and the effect of variations in n/B^2 will appear shortly in a separate publication by W.B. Thompson.

of the plasma from equations such as those given above since the exact motion depends on the linear combination of $\psi(r)\exp(i\omega t + im\phi)$ necessary to satisfy the initial conditions. To understand this in more tangible terms, a calculation has been performed by Wind and Sweetman using a simplified model in which the electron and ion clouds are assumed to be rigid rotating cylinders. The electron cloud is driven by a constant electric field due to the charge separation while the ion cloud is driven by a combination of the same field and the precessional drift about the magnetic axis. It is found that, for low densities, an initial displacement of the electrons results in a subsequent motion that is essentially $\frac{\vec{E} \times \vec{B}}{B^2}$ drift of the electrons cloud around the ion centre. The ion cloud is unable to move far from the axis because of the rapid $\frac{\vec{\nabla}B \times \vec{B}}{B^2}$ drift. This may correspond to the lower branch of Fig.12. An initial displacement of the ions allows a much more complicated motion. The fact that the frequency dependent mode of the oscillation appears always together with ion cyclotron emission is perhaps not surprising since it is known that the electrostatic instability at ion cyclotron frequency leads to a profound disturbance of the electron distribution.

3. Finite Larmor radius effects

Most of the finite Larmor radius effects have been taken into account in the derivation of the equation (6), such as the drift in the magnetic field represented by the velocity $\vec{v}_o$ (or $\vec{v}_D$), but the effect of the finite Larmor radius on the drifts produced by the electric field has not been taken into account completely. The fact that the ions see a variable electric field due to their drift velocity $\vec{v}_o$, apart from the explicit time dependence $\exp(i\omega t)$, has been taken into account by introducing the drift velocity $\frac{(\vec{v}_o \cdot \nabla)\vec{E}}{B\omega_c}$, which results in the automatic inclusion of the plasma dielectric constant $\varepsilon = 1 + \frac{4\pi Mc^2}{B^2} n$. However, the ions also have a velocity $\vec{V}$

around their centre of gyration and consequently there is an additional drift velocity arising from the fact that the electric field seen by the ions is different from that at the guiding centre. This drift velocity produces what is usually known as the finite Larmor radius effect.

We estimate the change in the drift velocity due to the finite Larmor radius by replacing the electric field at the guiding centre by its average around the Larmor orbit. An expansion of the electric field in powers of Larmor radius up to the second order is used for this purpose. This procedure corresponds to solving the equation of motion in a crossed magnetic and an inhomogeneous electric field accurate to the second order* It may be easily seen that the average electric field along the Larmor orbit is given by:-

$$\vec{E}\ (r,\phi) + \frac{a^2}{4}\ \nabla^2\ \vec{E}\ (r,\phi) + \ldots.$$

where (r,ϕ) are the co-ordinates of the guiding centre. The additional drift velocity $\vec{v}_L$ is then:-

$$\vec{v}_L = \frac{a^2}{4}\ \frac{\nabla^2\vec{E} \times \vec{B}}{B^2}$$

$$= \frac{-a^2}{4B}\left[\vec{r}_o\ \frac{im}{r}\ (\nabla^2\underline{\Psi}\ ) - \vec{\phi}_o\ \frac{\partial}{\partial r}\ (\nabla^2\underline{\Psi})\ \right]$$

This results in an additional term in the equation for Ψ (eqn.(6)) of the form:-

$$\frac{4\pi M c n_o^2}{B^2}\ \frac{\kappa k V^2 (1 - 3\delta)}{4\omega_c (\omega + m\Omega)}\ \nabla^2\ \underline{\Psi}$$

The equation (6) can now be corrected by replacing ε by:-

$$\varepsilon' = \varepsilon + \frac{4\pi M c^2 n}{B^2}\ \frac{\kappa k V^2 (1 - 3\delta)}{4\omega_c (\omega + m\Omega)}$$

and the full equation for the electric potential including the first

---

* W.B. Thompson, private communication.

order finite Larmor radius effect becomes the following:-

$$\left[1 + \frac{4\pi Mc^2 n_o}{B^2}\left(1 + \frac{\kappa V^2 k(1-3\delta)}{4\omega_c(\omega+m\Omega)}\right)\right]\frac{d^2\psi}{dr^2} + \left[\frac{1}{r} + \frac{4\pi Mc^2}{B^2}\frac{dn_o}{dr}\left\{(1-2\delta) + \frac{V^2k^2(1-3\delta)}{4m\omega_c(\omega+m\Omega)}\right\}\right]\frac{d\psi}{dr}$$

$$+ \left[\frac{-4\pi ec}{\omega(\omega+m\Omega)Br}\frac{dn_o}{dr}\left(m^2\Omega + \frac{V^2k^2(1-3\delta)m\omega}{4\omega_c^2}\right) - \frac{m^2}{r^2}\right]\psi = 0 \qquad \ldots.(14)$$

We can now check our assumption $\varepsilon' = 1$, which was made implicitly in applying equation (7) to the experiment. Approximating ω by $\frac{-\Omega}{2}$ and setting $m = 1$, we find that ε' differs from unity by 6% to 20% in the region between 40 kG to 10 kG, and that the difference increases rapidly below 10 kG becoming over 60% at 5 kG. These figures are calculated for an experimentally reached density of 3×10^8 particles/c.c. Since the equation (14) has not yet been solved, the exact importance of the finite Larmor radius term is not known. However, the fact that ε' begins to differ markedly from unity below about 10 kG and at densities above a few times 10^8 particles/c.c. may be regarded as an indication that the finite Larmor radius effect could begin to be important.

V. CONCLUSIONS

We have observed experimentally strong emission at the ion cyclotron and related frequencies at densities where $\omega_{p_e} > \omega_{c_i}$. This, together with the strong axial motion of the electrons observed, tends to indicate an unstable longitudinal electrostatic oscillation which arises from the strong anisotropy of the velocity distribution. This type of instability has been extensively studied by Harris, and others. The emission of ion cyclotron radiation has been observed to be either self-quenching or continuous depending on the density and magnetic field. The self-quenching phenomena may be connected to the strong scattering of ions out of the transverse plane during the instability, as this reduces the anisotropy of the distribution.

This aspect of the problem has not so far been considered theoretically, although experimentally much information on these lines may be obtained.

It is interesting to note that the plasma is apparently stable to this instability at all investigated densities and magnetic fields below about 12 kG. A recent calculation of Harris[19] which takes full account of ion and electron distributions but assuming a cylindrical shell of plasma indicate that the plasma may be stable at all densities provided ω_c is sufficiently small. Although this calculation is not strictly applicable to the present case where Larmor orbits are overlapping, it may be conjectured that a similar conclusion can be drawn. This would agree with the experimental observation and may point towards a way of eliminating the instability altogether in future experiments.

A major obstacle to the attainment of higher density is presented by the m = 1 low frequency instability which in this case is induced by charge separation due to the ion precessional drift in mirror magnetic field. The growth of the instability is limited by the physical presence of a radial probe and an equilibrium situation is set up when the amount of plasma supplied by the injection current is equal to that removed by the probe. The density is thus limited at $\sim 3 \times 10^8$ particles/c.c. for fields above 20 kG. This order of density appears to be the limit in all present day high energy injection simple mirror systems. It is interesting to note that we have observed two kinds of frequency dependence on density, both for m = 1 charge separation. Both the density dependent and density independent oscillations have also been observed in the Alice experiment[4]. However, we have not observed frequencies much above $\frac{1}{2}$ the ion precession frequency, whereas in the Alice experiment frequencies at and above the ion precession frequency have been observed. We have shown that the infinite plane plasma calculation is grossly

inadequate when applied to a plasma of cylindrical shape by writing $k = \frac{1}{r_o}$, the predicted stability boundary is two orders of magnitude too low. Although the finite Larmor radius effect is taken into account in this calculation, the fact that the electric field is assumed to be varying only in the direction of wave propagation essentially invalidates its application to a cylindrical plasma.

In the present calculation, where the cylindrical plasma and the boundary conditions are properly taken into account, the stability boundary prediction agrees quite well with experiment above 20 kG. The variation of frequency with density is also quite well explained although it is not understood why frequencies above $\frac{\omega_i}{2}$ have not been observed. It has been found that the electric field inside the plasma cannot be uniform. This means that finite Larmor effect can be expected for m = 1, contrary to the conclusion of R.K. and R. The complete equation for the electric potential including first order finite Larmor radius effect shows that at densities above 10^8 particles/c.c. and magnetic fields below about 10 kG, the finite Larmor radius could be expected to play an important role. This may explain the extremely sharp rise in the stability boundary at 15 kG observed experimentally (Fig.8). However the exact effect of the finite Larmor radius term cannot be predicted until equation (14) is solved.

ACKNOWLEDGEMENTS

We should like to express our warmest thanks to Mr. R.E. Bradford, Mr. J. Coupland and the members of the Phoenix running team for their invaluable assistance in the experimental work and to Professor W.B. Thompson for his invaluable inspiration and guidance throughout the theoretical development.

REFERENCES

1. M.N. Rosenbluth and C.L. Longmire, Ann. Phys.(N.Y.) 1, 120 (1957)

2. M.N. Rosenbluth, N.A. Krall and N. Rostoker, Nuclear Fusion,1962 Supplement, Part 1, 143, (1962).

3. A.B. Mikhailovskii, Zhur. Eksp. i Teoret. Fiz. 43, 509 (1962) or Soviet Phys. - JETP, 16, 364 (1963).

4. C.C. Damm, J.H. Foote, A.H. Futch and R.F. Post, Phys. Rev. Letters, 10, 323, (1963).

5. G.F. Bogdanov, I.N. Golovin, Yu. A. Kucheryaev and D.A. Panov, Nuclear Fusion, 1962 Supplement, Part 1, 215, (1962).

6. W.A. Perkins and R.F. Post, Observation of plasma instability with rotational effects in a mirror machine, University of California, Lawrence Radiation Laboratory, Livermore, Report UCRL - 7302, (1963).

7. M.S. Ioffé, R.I. Sobolev, V.G. Telkovskii and E.E. Yushmanov, U.S.A.E.C. Translation, AEC - tr - 4217, (1960).

8. E.G. Harris, Phys. Rev. Letters, 2, 34 (1959).

9. E.G. Harris, Unstable plasma oscillations in a magnetic field, Oak Ridge National Laboratory, Report ORNL-2728 (1959)

10. P.R. Bell et al., Oak Ridge National Laboratory, Thermonuclear Division, Semiannual progress report for period ending October 31st, 1962. ORNL-3392, 11, (1963).

11. D.R. Sweetman, Nuclear Fusion, 1962 Supplement, Part 1, 279, (1962).

12. F.D. Kahn. To be published.

13. Yu. N. Dnestrovsky, D.P. Kostomarov and V.I. Pistunovich, Nuclear Fusion, 3, 30 (1963).

14. N.A. Krall and M.N. Rosenbluth, Phys. Fluids, 4, 163 (1961).

15. N.A. Krall and M.N. Rosenbluth, Phys. Fluids, 5, 1435 (1962).

16. M.N. Rosenbluth and N.A. Krall, Phys. Fluids, 6, 254 (1963).

17. B.B. Kadomtsev, Soviet Phys. - JETP, 13, 223, (1961).

18. E. Jahnke and F. Emde, Tables of Functions, 4th ed., Dover Publications, New York (1945).

19. E.G. Harris, The effect of finite ion and electron temperatures on the ion cyclotron resonance instability, Culham Laboratory report CLM - R32 (1963).

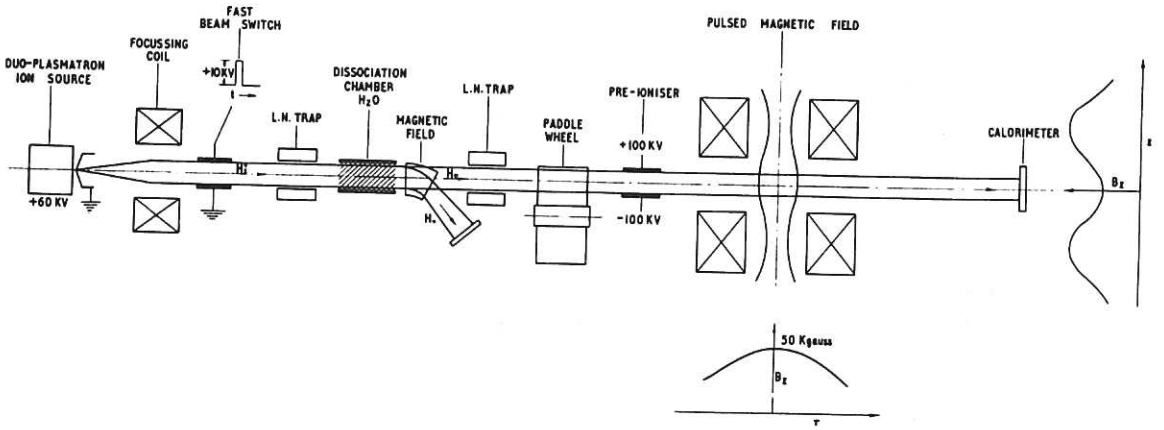

CLM-P 32 Fig. 1
Schematic diagram of PHOENIX

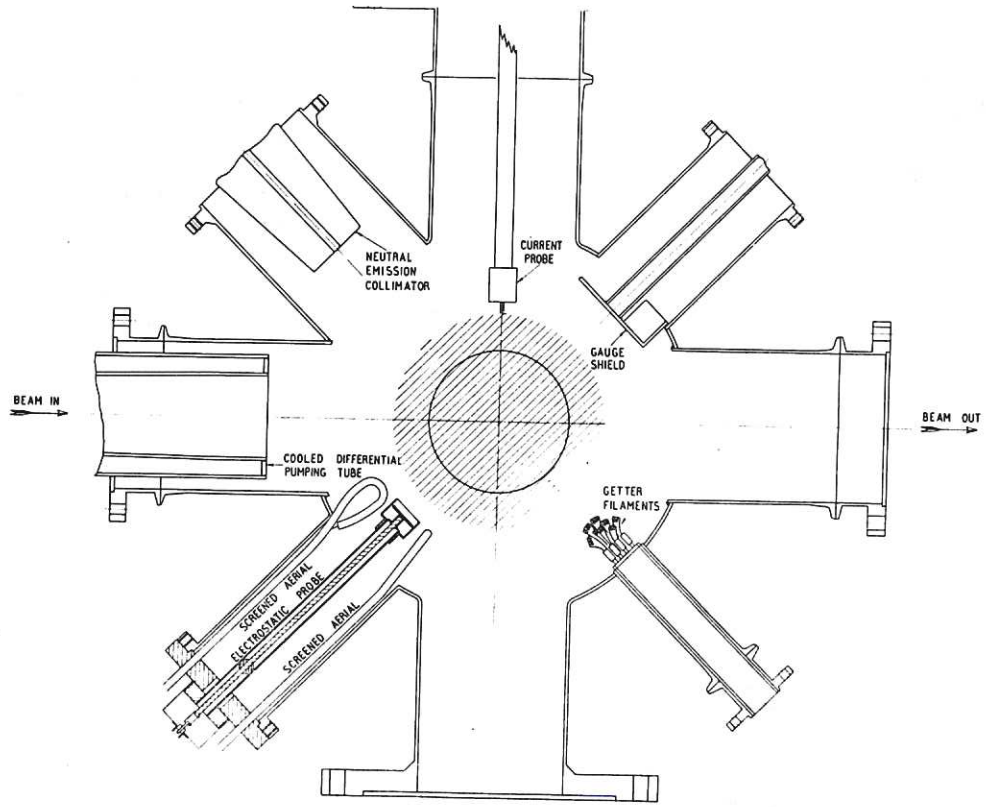

CLM-P 32 Fig. 2
Schematic section through the median plane of PHOENIX showing the diagnostic arrangements.

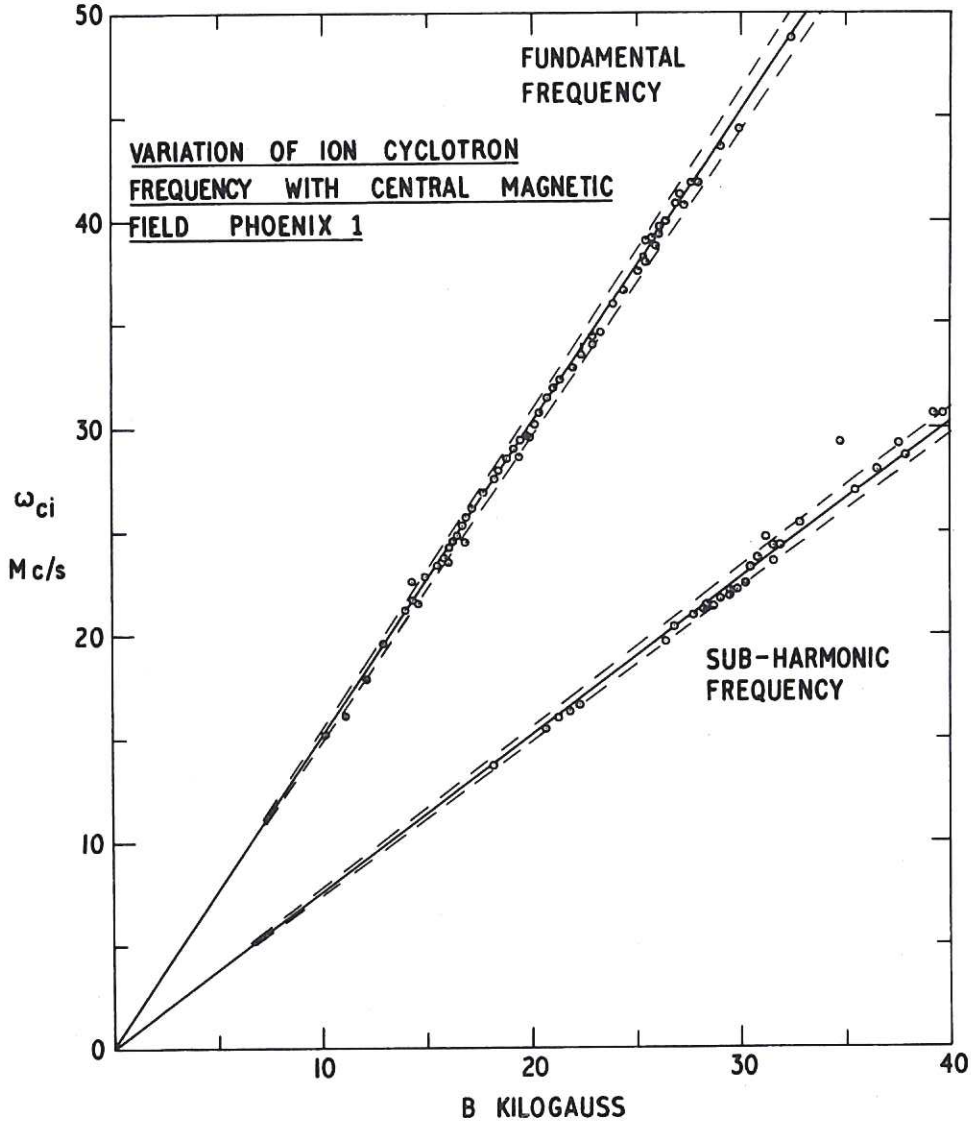

CLM-P32 Fig. 3

Variation of ion cyclotron frequency with central magnetic field. The circles are experimental points, the straight lines are calculated from

$$\omega_c = \frac{eB}{m_i c} \text{ and } \frac{1}{2}\frac{eB}{m_i c}$$

The dashed lines indicate the uncertainty in the determination of the magnetic field.

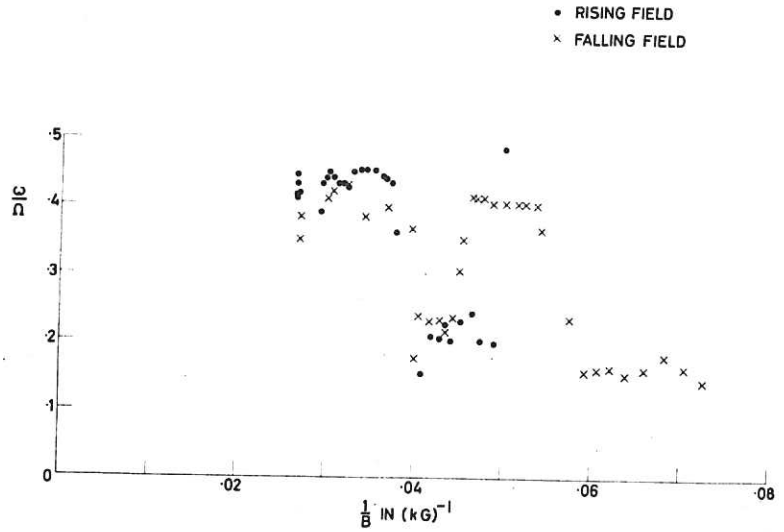

CLM-P 32 Fig. 4

The ratio of observed frequency ω upon ion precession frequency, Ω, calculated at 7 cm radius, is plotted against the inverse of the central magnetic field B. Circles indicate points taken during the rising part of the field cycle and crosses indicate points taken during the falling part of the field cycle.

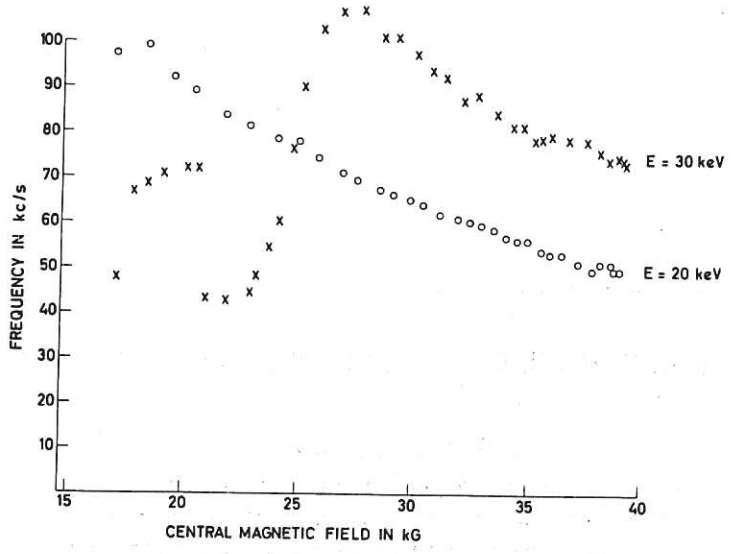

CLM-P 32 Fig. 5

The variation of observed frequency with central magnetic field for two ion energies 30 keV and 20 keV.

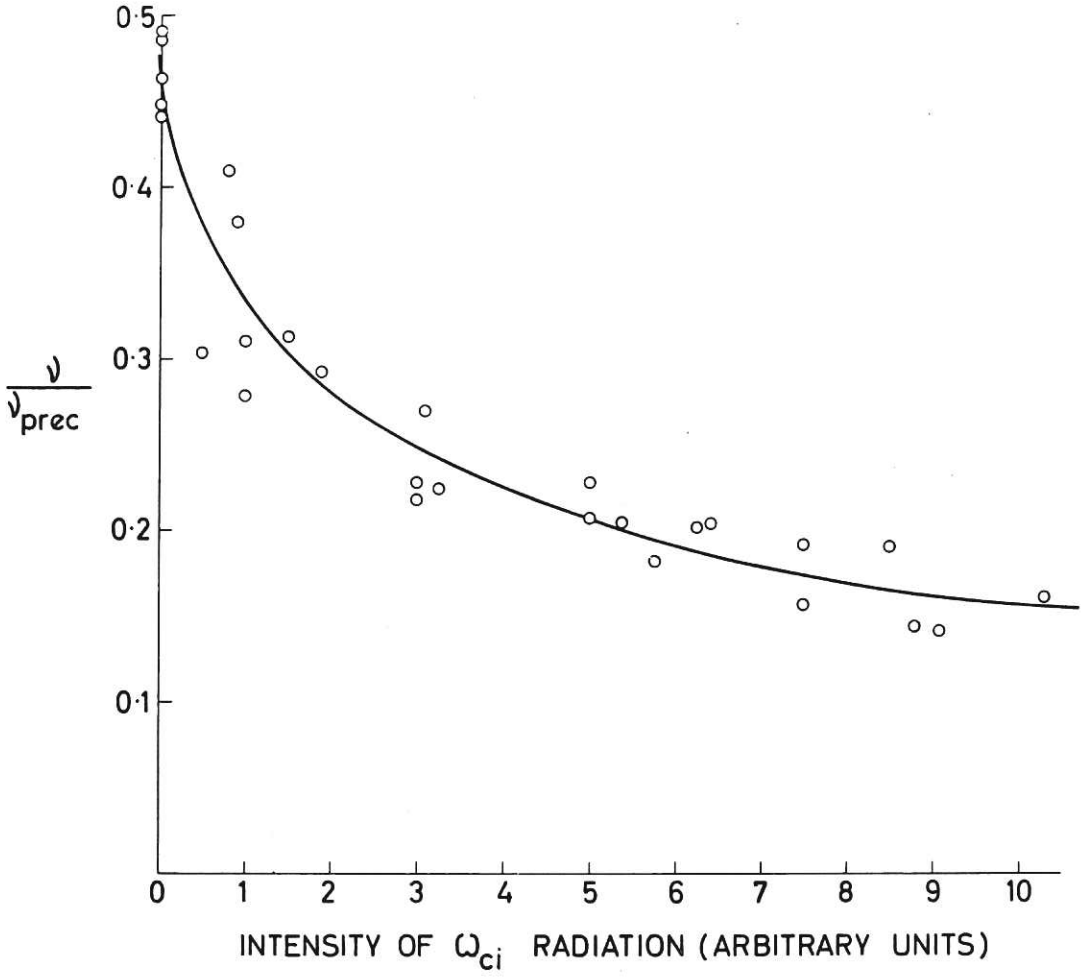

CLM-P 32 Fig. 6

The variation of frequency, plotted as the ratio of observed frequency ω to ion precession frequency Ω at 7 cm radius, with the intensity of measured ion cyclotron emission. The circles are experimental points obtained from five pulses.

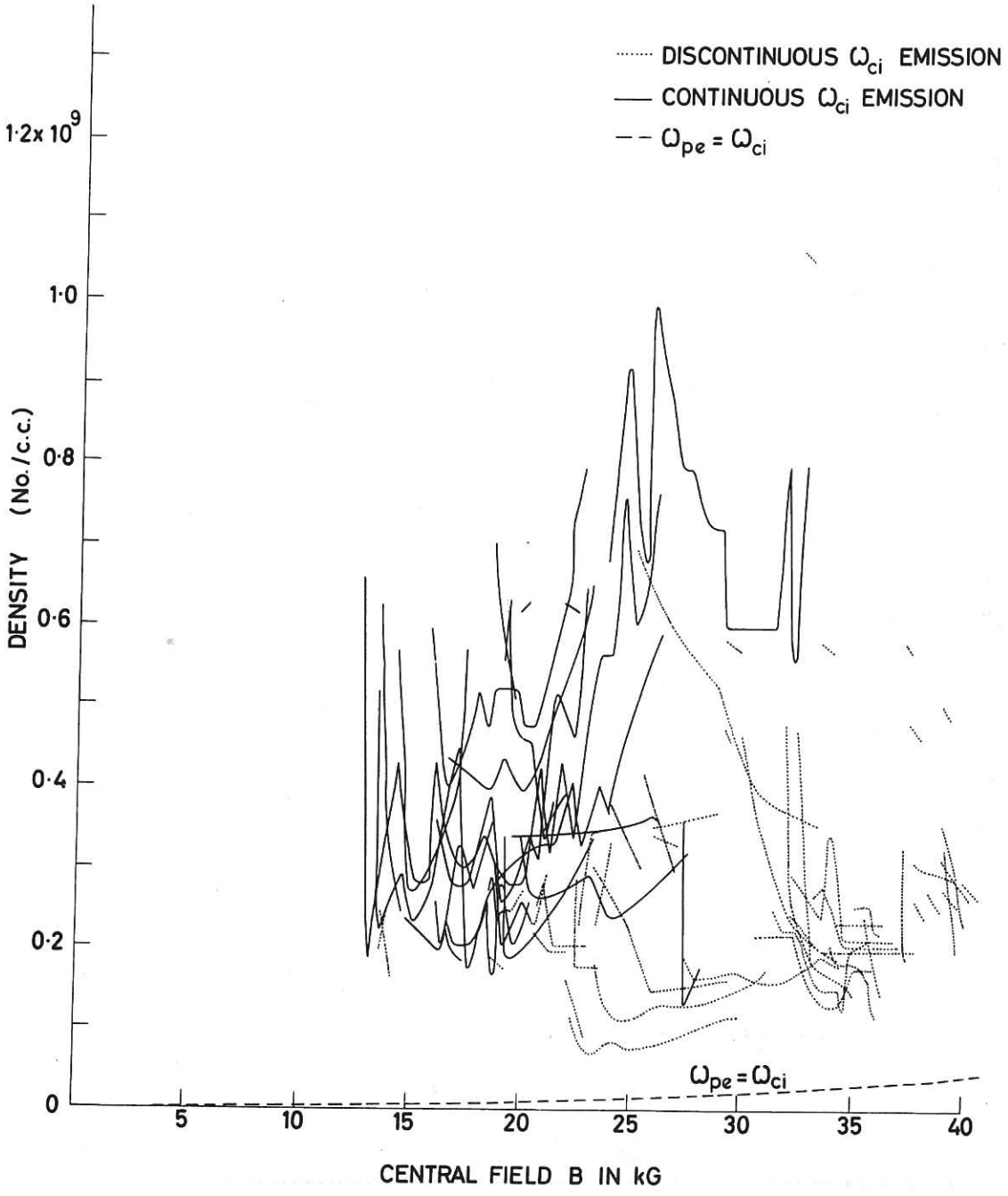

CLM-P 32 Fig. 7

A superposition of results of many pulses showing regions on the density vs magnetic field plot where continuous and discontinuous ion cyclotron emission occur. The dashed line indicates the theoretical limit above which unstable longitudinal electrostatic oscillations may occur.

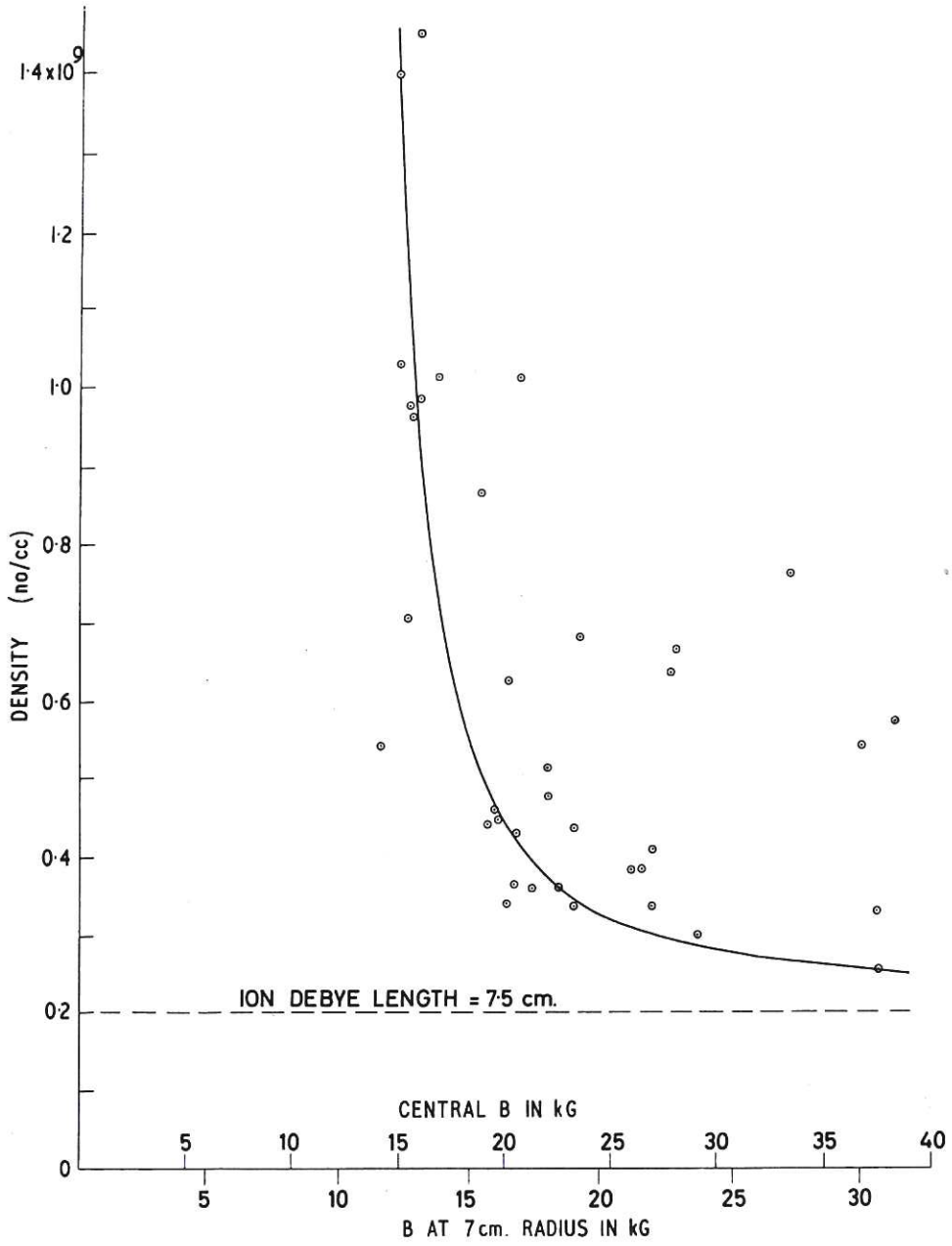

CLM-P32 Fig. 8

The onset of low frequency oscillations seen on a density vs magnetic field plot. Each circle indicates the density and magnetic field at which low frequency oscillations start in each pulse. Both the magnetic field and density are increasing with time starting at zero at the beginning of the pulse. A line is drawn in to separate the stable and unstable regions.

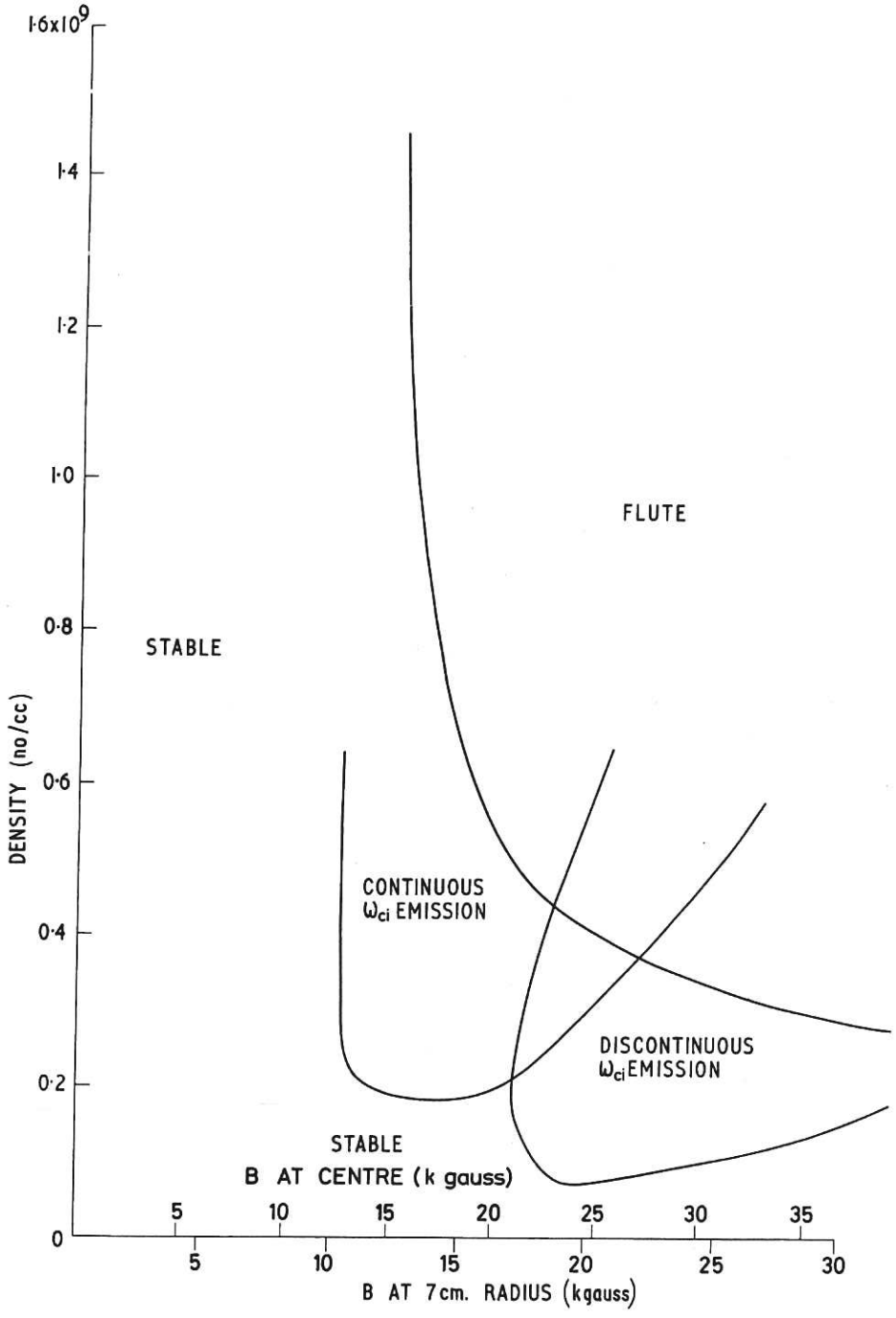

CLM-P 32 Fig. 9

Schematic diagram showing the different regions of instability on a density vs magnetic field plot.

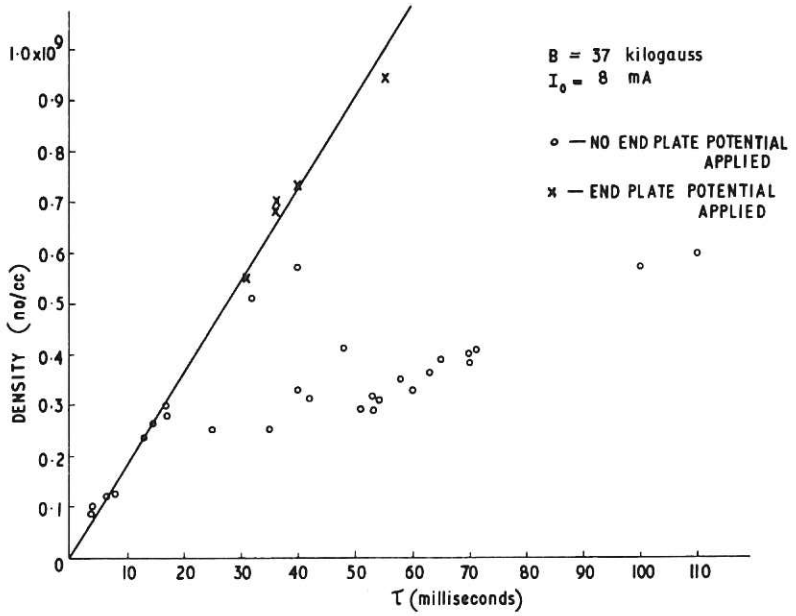

CLM-P 32 Fig. 10

Plasma density, n^+, at 37 kG against plasma decay time τ showing the limiting effect of low frequency instability and the effect of end plate potentials. The circles are experimental points with no end plate potentials and crosses are with end plate potentials. The solid line is calculated from $n^+ \propto \tau j$.

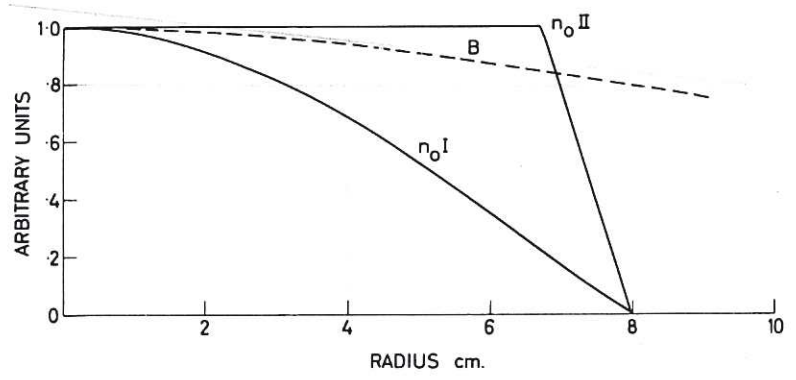

CLM-P 32 Fig. 11

The magnetic field and density profiles assumed in the calculations. The curve marked B shows the assumed magnetic field profile which is a convenient and close approximation to the magnetic field profile in PHOENIX. The curve marked n_0 I shows the density profile given by eqn. (8). The curve marked n_0 II shows the density profile defined by eqn. (12), for the case where B_0 = 36 kG.

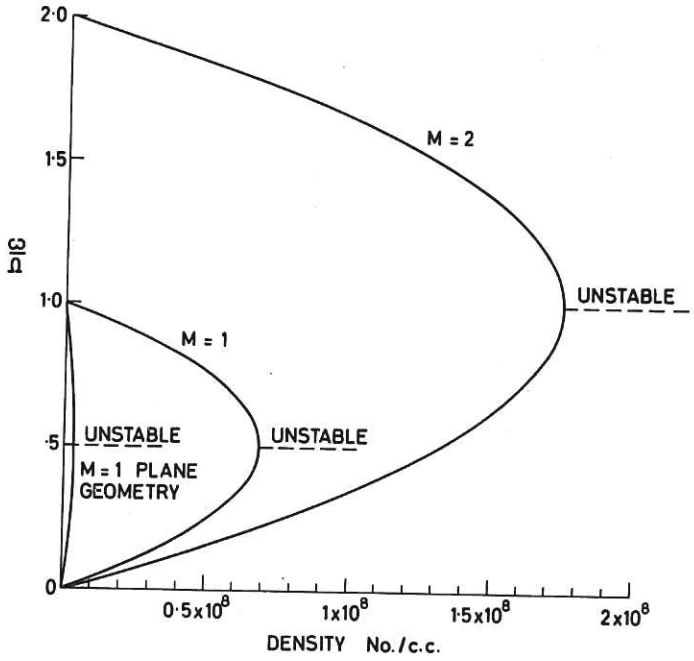

CLM-P 32 Fig. 12

The variation of oscillation frequency, plotted as the ratio of observed frequency upon ion precession frequency, with density. The curves for m = 1 and m = 2 modes have been calculated from eqn. (10) using density profile $n_0 I$. The dashed lines mark the frequencies of the unstable waves. The curve marked 'plane geometry' has been obtained from Mikhailovskii using $k = 1/r_0$ (eqn. (3).) This curve applies both for cases with and without finite Larmor radius correction.

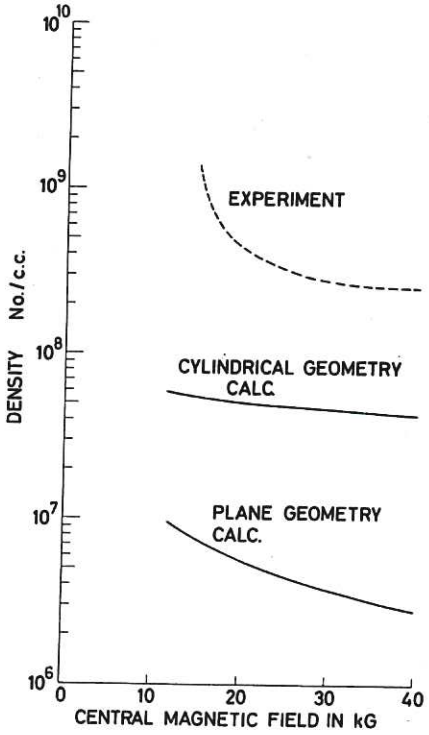

CLM-P 32 Fig. 13

Stability boundary on the density vs magnetic field plot. The line marked 'experimental' has been taken from Fig. 8. The line marked 'cylindrical geometry calc.' has been obtained from the calculation indicated in eqn. (12) The width of the shell was one Larmor diameter and therefore is a function of magnetic field. The line marked 'plane geometry calc.' has been obtained by calculation indicated in eqn. 3. The line remains essentially unchanged for both with and without finite Larmor radius correction.